Institute of Physics Publishing Journal of Physics: Conference Series **11** (2005) 169–179
doi:10.1088/1742-6596/11/1/017 Kinetic Theory of Nonideal Plasmas

Irreversible energy gain by linear and nonlinear oscillators

D Bauer[1] **and P Mulser**[2]

[1]Max-Planck-Institut für Kernphysik, Postfach 103980, 69029 Heidelberg, Germany

[2]Theoretical Quantum Electronics (TQE), TU Darmstadt, Schlossgartenstr. 7, 64289 Darmstadt, Germany

E-mail: peter.mulser@physik.tu-darmstadt.de

Abstract. A particle can gain appreciable irreversible energy ("absorption") from linear or nonlinear oscillations only by ballistic excitation ("collision") or, if excited by an adiabatic pulse of constant frequency, by undergoing resonance. For the linear oscillator it is shown that the transition from ballistic to adiabatic behavior out of resonance occurs for $\sin^2$-pulses 2–4 eigenperiod long. In the case of a linear oscillator with time-varying eigenfrequency it is shown that Cornu's double spiral represents an attractor, either for zero energy gain out of resonance or finite gain by transiting through resonance. One of the remarkable properties of nonlinear oscillators is that resonance depends on the level of excitation. It is this property which opens a new access to understanding the dominant heating process at high laser intensities, the so-called collisionless absorption phase in solids, extended cluster media, dusty plasmas, and sprays, well guaranteed by experiments and computer simulations but hitherto not well understood in physical terms.

.

1. Introduction

Coupling of radiation to plasma is, except special conditions, mediated by the elctrons. The optical properties, like propagation and diffraction, scattering of radiation, and absorption are calculated from single particle models where the single particle is a bare electron in an ideal plasma and a quasielectron in a nonideal, i.e., strongly coupled plasma. In this framework the most commonly used model is that of a driven linear or nonlinear oscillator or, such an oscillator model constitutes an equivalent alternative to describe the phenomenon under investigation. When dealing with a fully ionized plasma in which the electrons are free to move, one may miss the restoring force. In fact, collisional absorption in a plasma for example is well described by means of a generalized Drude model of the structure

$$\frac{\mathrm{d}\boldsymbol{v}_e}{\mathrm{d}t} + \nu \boldsymbol{v}_e = -\frac{e}{m_e}\boldsymbol{E} \tag{1}$$

where the damping coefficient ν depends on the frequency ω of the driving field (an intense laser field, for instance), on the kinetic electron temperature T_e, and the driver field amplitude $\hat{\boldsymbol{E}}$, i.e., $\nu = \nu(\omega, T_e, \hat{\boldsymbol{E}})$. In principle (1) is a damped oscillator with zero eigenfrequency. The damping coefficient ν is a phenomenological parameter. As soon as a description on a more fundamental level, in the extreme case on a rigorous kinetic level is chosen, it is very likely that an oscillator equation with finite eigenfrequency and free of damping comes about again. To give an example, collisional absorption of a parallel stream of monoenergetic electrons of velocity $\boldsymbol{v}_0$ in the dielectric approach is described by the linear oscillator equation for the electron displacement $\boldsymbol{\delta}$,

$$\ddot{\boldsymbol{\delta}} + \omega_p^2 \boldsymbol{\delta} = \boldsymbol{f}_C(\boldsymbol{v}_0, t). \tag{2}$$

Here, the driving term is the Coulomb force $\boldsymbol{f}_C$ of a bare charge (for example an ion) and the plasma frequency ω_p provides for screening. The finite eigenfrequency and the absence of damping reflect the facts that free electrons in a plasma are always exposed to their own space charge fields and that the quantum or classical equations of motion are reversible. In the case of (2) the amplite $\hat{\boldsymbol{\delta}}$ is a function of the impact parameter b, $\hat{\boldsymbol{\delta}} = \hat{\boldsymbol{\delta}}(b)$, and it can be shown that excitation becomes negligible for $b > v_0/\omega_p$, or in other words, when the interaction time is longer than $\tau = 2/\omega_p$, i.e., approximately one third of the eigenperiod $T_0 = 2\pi/\omega_p$ [1]. If a force $\boldsymbol{f}_C$ of halfwidth larger than $T_0/3$ acts on the oscillator (2) the oscillator reacts adiabatically, i.e., the interaction is reversible; a collision lasting longer than $T_0/3$ is no longer a collision.

With the application of ultrashort intense laser pulses to create dense plasmas by heating solid matter, extended cluster media, dusts and aerosols so-called collisionless laser light absorption has shown to play an important role. Its existence is well proved in experiments and by computer simulations [2, 3], however until recently the underlying physical mechanism leading to irreversibility was not understood. Progress in analyzing the phenomenon has been made by studying the excitation of nonlinear oscillators governed by an equation of the type

$$\ddot{\boldsymbol{x}} + \boldsymbol{f}(\boldsymbol{x}) = \boldsymbol{a}(t) \tag{3}$$

where $\boldsymbol{f}(\boldsymbol{x})$ is any sufficiently smooth restoring force, and $\boldsymbol{a}(t)$ is an external driver. The linear oscillator is described by $\boldsymbol{f}(\boldsymbol{x}) = \omega_0^2\boldsymbol{x}$ with constant eigenfrequency ω_0 at all excitation amplitudes. Under the action of a harmonic driver $\boldsymbol{a}(t) = \hat{\boldsymbol{a}}(t)\cos\omega t$, $\omega \neq \omega_0$, it behaves adiabatically as soon as $\hat{\boldsymbol{a}}(t)$ is an envelope of several cycles $T = 2\pi/\omega$ long, whereas it continues to oscillate indefinitely (net energy absorption) if $\hat{\boldsymbol{a}}(t)$ is δ-peak like.

In this paper we investigate (i) the transition from collisional to adiabatic behavior of the oscillator (3) as a function of the length of the envelope $\hat{\boldsymbol{a}}$ and (ii) under which conditions irreversible energy gain (absorption) can take place under the action of long pulses $\hat{\boldsymbol{a}}(t)$. As it will be shown this last step will be the key to understanding collisionless absorption out of linear resonance.

2. Excitation of the linear oscillator

For orientation and to make the behavior of the nonlinear oscillator (3) more understandable it is advisible to study first the collisional and adiabatic excitation modes of the linear oscillator with constant ω_0 and time-varying ω_0, $\omega_0 = \omega_0(t)$. The one-dimensional oscillator

$$\ddot{x} + \omega_0^2 x = \hat{a}(t)\cos\omega t \tag{4}$$

under the initial condition $x(-\infty) = \dot{x}(-\infty) = 0$, $\hat{a}(-\infty) = 0$ evolves in time according to

$$x(t) = \frac{\sin\omega_0 t}{\omega_0}\int_{-\infty}^{t} \hat{a}(t')\cos\omega_0 t'\cos\omega t'\,\mathrm{d}t' - \frac{\cos\omega_0 t}{\omega_0}\int_{-\infty}^{t} \hat{a}(t')\sin\omega_0 t'\cos\omega t'\,\mathrm{d}t'. \tag{5}$$

For $\hat{a}(t) = \omega_0 x_0 \delta(t)$ the ballistic solution $x(t > 0) = x_0 \sin\omega_0 t$ results. The general solution can be cast into the form

$$x(t) = \frac{\sin\omega_0 t}{2\omega_0}\int_{-\infty}^{t} \hat{a}(t')[\cos\omega_1 t' + \cos\omega_2 t']\,\mathrm{d}t' - \frac{\cos\omega_0 t}{2\omega_0}\int_{-\infty}^{t} \hat{a}(t')[\sin\omega_1 t' + \sin\omega_2 t']\,\mathrm{d}t'. \tag{6}$$

where $\omega_1 = \omega_0 + \omega$ and $\omega_2 = \omega_0 - \omega$. For laser interaction with solid density matter $\omega \ll \omega_0$ can be chosen. With a rectangular excitation amplitude $\hat{a}(t) = \omega_0^2 x_0$, centered around $t = 0$ and $\Delta t = 2t_0$ long,

$$x(t \geq t_0) = 2x_0 \sin\omega_0 t_0 \sin\omega_0 t \tag{7}$$

results.

Maximum irreversible energy gain is achieved with exciting pulses of length $\Delta t \approx \pi/\omega_0 = 2T_0 \ll T = 2\pi/\omega$. Alternatively, if $\hat{a}(t)$ is a smooth function of halfwidth $\Delta t/2 = t_0 \gtrsim T$ integration by parts of (6) with suitable test functions $\hat{a}(t)$ shows that the irreversible energy gain $e_a(t = \infty)$ compared to the maximum oscillatory energy $e_{\max}$ during the pulse is much less than unity. In Fig. 1 the transition of $e_a(t > t_0)$ from ballistic to adiabatic excitation of (4) is shown at $\omega_0 = \omega$ (solid), $\omega_0 = 2\omega$ (dotted), and $\omega_0 = 10\omega$ (dashed) as a function of the number of exciting ω-cycles n for $\hat{a}(t) = a_0 \sin^2[\omega t/(2n)]$ in the interval $0 < \omega t/(2n) < \pi$ and zero outside. It is seen that far from resonance ballistic excitation with finite irreversible gain $e_a(t \to \infty)$ is achieved with very short pulses only. To save 1% of the maximum $e_a(t \to \infty)$, reached with pulses of length $0.1T = T_0$ for $\omega_0 = 10\omega$ and $0.7T = 1.4T_0$ for $\omega_0 = 2\omega$, the exciting pulse length must not exceed $0.2T$ and $1.9T$, respectively. For comparison the energy gain at resonance $\omega_0 = \omega$ is also plotted. It resembles the quadratic time dependence of the energy gain at constant amplitude.

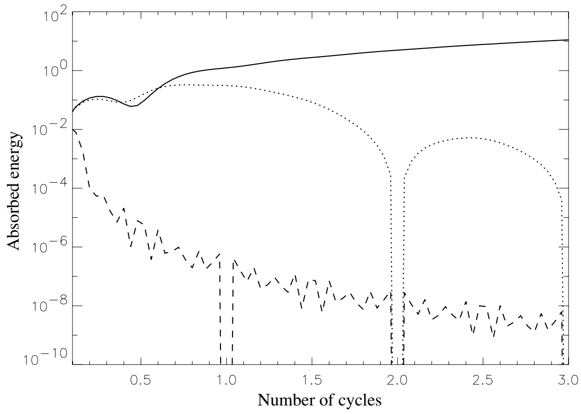

Figure 1. Ballistic vs adiabatic excitation of the linear oscillator (4). Absorbed energy in units of $(a_0/\omega)^2$ from a $\sin^2$-pulse, n cycles long; dashed: $\omega_0 = 10\omega$, dotted: $\omega_0 = 2\omega$. Maximum irreversible energy gain is achieved with pulses of length $0.1T = T_0$ for $\omega_0 = 10\omega$ and $0.7T = 1.4T_0$ for $\omega_0 = 2\omega$ (ballistic excitation). The higher the detuning q, $\omega_0 = q\omega$, the faster drops the energy gain with increasing pulse duration (adiabatic behavior). For comparison the energy absorption at resonance $q = 1$ is also shown (solid).

Next we consider the linear oscillator with time varying eigenfrequency $\omega_0(t)$,

$$\ddot{x} + \omega_0^2(t)x = \hat{a}\cos\omega t, \qquad \omega_0(t) = \omega \mathrm{e}^{-\alpha t}, \quad \alpha > 0. \tag{8}$$

It is a model for linear as well as nonlinear resonance absorption and wave breaking with nanosecond lasers [4]. The driver is adiabatically switched on at $t = -\infty$ and held constant in the interval of interest. The eigenfrequency varies from $\omega_0(-\infty) = \infty$ to $\omega_0(+\infty) = 0$. Highest excitation is expected for $\alpha \ll \omega$, i.e., when the oscillator remains close to resonance $\omega_0(t = 0) = \omega$ for a time as long as possible. Under $\alpha \ll \omega$ the functions $\sin\phi$ and $\cos\phi$,

$$\phi = \int_0^t \omega_0(t')\,\mathrm{d}t' = \frac{\omega}{\alpha}\left(1 - \mathrm{e}^{-\alpha t}\right), \qquad \ddot{\phi} = -\alpha\omega_0 \gg -\omega_0^2, \tag{9}$$

represent two independent solutions of the homogeneous oscillator equation (8) to a satisfactory approximation. Hence the desired solution of (8) with $x(-\infty) = \dot{x}(-\infty) = 0$ is

$$x(t) \approx \hat{a}\left\{\sin\phi(t)\int_{-\infty}^t \frac{\cos\phi(t')}{\omega_0(t')}\cos\omega t'\,\mathrm{d}t' - \cos\phi(t)\int_{-\infty}^t \frac{\sin\phi(t')}{\omega_0(t')}\cos\omega t'\,\mathrm{d}t'\right\}. \tag{10}$$

This expression becomes an exact solution if on the RHS of (8) the term

$$y(t) = \ddot{\phi}\hat{a}\left\{\cos\phi(t)\int_{-\infty}^t \frac{\cos\phi(t')}{\omega_0(t')}\cos\omega t'\,\mathrm{d}t' + \sin\phi(t)\int_{-\infty}^t \frac{\sin\phi(t')}{\omega_0(t')}\cos\omega t'\,\mathrm{d}t'\right\} \tag{11}$$

is added. The amplitude $\hat{x}(t)$ of $x(t)$ is expected to grow appreciably only in a narrow interval $\Delta\omega_0$ around the resonant point $t = 0$. Therefore, under the integral (and only there) $\omega_0(t)$ and $\phi(t)$ can be expanded to lowest order,

$$\omega_0(t) = \omega\mathrm{e}^{-\alpha t} \approx \omega(1 - \alpha t), \qquad \phi(t) \approx \omega(t - \alpha t^2/2). \tag{12}$$

By observing that $\cos\phi\cos\omega t = [\cos(\phi+\omega t)+\cos(\phi-\omega t)]/2$, $\sin\phi\cos\omega t = [\sin(\phi+\omega t)+\sin(\phi-\omega t)]/2$ the terms containing $\cos(\phi+\omega t)$ and $\sin(\phi+\omega t)$ can be omitted since they merely lead to fast low-amplitude modulations, whereas the two terms containing $\phi-\omega t$ exhibit a stationary phase around $\omega_0 = \omega$. This is analoguous to the rotating wave approximation in the magnetic and optical Bloch models. Further, $\omega_0(t)$ can be taken out of the integrals. Then $x(t)$ from (10) reads in the resonance region

$$x(t) \approx \frac{\hat{a}}{2\omega}\left\{\sin\phi(t)\int_{-\infty}^{t}\cos\frac{\alpha}{2}\omega t'^2\,\mathrm{d}t' + \cos\phi(t)\int_{-\infty}^{t}\sin\frac{\alpha}{2}\omega t'^2\,\mathrm{d}t'\right\}. \tag{13}$$

By the substitution $t = [\pi/(\alpha\omega)]^{1/2}\eta$ it transforms into

$$x(\eta) \approx \frac{\pi^{1/2}\hat{a}}{2\alpha^{1/2}\omega^{3/2}}\left\{\left[\frac{1}{2}+C(\eta)\right]\sin\phi(\eta) + \left[\frac{1}{2}+S(\eta)\right]\cos\phi(\eta)\right\}, \tag{14}$$

with the Fresnel integrals [5]

$$C(\eta) = \int_0^{\eta}\cos\frac{\pi}{2}\eta'^2\,\mathrm{d}\eta', \qquad S(\eta) = \int_0^{\eta}\sin\frac{\pi}{2}\eta'^2\,\mathrm{d}\eta'. \tag{15}$$

For $\eta \to \infty$ they behave as

$$C(\eta) = \frac{1}{2} + \frac{1}{\pi\eta}\sin\frac{\pi}{2}\eta^2 + O(\eta^{-2}), \qquad S(\eta) = \frac{1}{2} - \frac{1}{\pi\eta}\cos\frac{\pi}{2}\eta^2 + O(\eta^{-2}).$$

Solution (14) can be expressed in terms of amplitude and phase,

$$x(\eta) \approx \hat{x}(\eta)\sin[\phi(\eta)+\psi(\eta)], \tag{16}$$

$$\hat{x}(\eta) = \frac{\pi^{1/2}\hat{a}}{2\alpha^{1/2}\omega^{3/2}}\left\{\left[\frac{1}{2}+C(\eta)\right]^2 + \left[\frac{1}{2}+S(\eta)\right]^2\right\}^{1/2}, \quad \psi(\eta) = \arctan\left(\frac{S(\eta)+1/2}{C(\eta)+1/2}\right) + \psi_0.$$

The plot of $I(\eta) = C(\eta) + \mathrm{i}S(\eta)$ in the complex plane yields the familiar Cornu spiral, Fig. 2, well known from diffraction theory in classical optics. The path s along the spiral from the origin to a point $P = C(\eta) + \mathrm{i}S(\eta)$ is the parameter η itself, $s(\eta) = \eta$, the amplitude $A(\eta) = \{[1/2 + C(\eta)]^2 + [1/2 + S(\eta)]^2\}^{1/2}$ is the length of the arrow pointing from $O' = -(1/2 + \mathrm{i}/2)$ to $P = C(\eta) + \mathrm{i}S(\eta)$. The resonance width and the factor of amplitude growth are conveniently defined by the change of phase $\psi(\eta)$ from $\psi_0 - \pi/2$ to $\psi_0 + \pi/2$ and $S(\eta) = C(\eta)$ (see arrows in Fig. 2). This is the case for $\eta = \eta_r = 1.27$ and $\eta = -\eta_r$, respectively. According to (14) the resonance interval and frequency halfwidth are

$$\omega + \Delta\omega_0 \geq \omega_0 \geq \omega - \Delta\omega_0, \qquad \frac{\Delta\omega_0}{\omega} = (\pi\alpha)^{1/2}\eta. \tag{17}$$

The resonance interval $2\Delta\omega_0$ increases as $\alpha^{1/2}$ and covers the number of oscillations

$$N = \frac{2t_r}{2\pi/\omega} = \left(\frac{\omega}{\pi\alpha}\right)^{1/2}\eta_r. \tag{18}$$

For $\alpha = \omega/100$ and $\alpha = \omega/10$ results $N = 7.2$ and $N = 2.3$. The associated resonance halfwidths are $\Delta\omega_0/\omega = 0.23$ and $\Delta\omega_0/\omega = 0.7$. In general the quantities $x(t)$ and $y(t)/\ddot{\phi}$ from (10) and (11) are of the same magnitude. Therefore $x(t)$ is expected to be a good approximation if $(\alpha/\omega)^{1/2} \ll 1$ is fulfilled. The same restriction follows also from (17) for the validity of expansion (12). From the numerical examples above for $\Delta\omega_0/\omega$ one sees that with $\alpha/\omega = 10^{-2}$ the two quantities $\exp(-\alpha t_r)$ and $(1-\alpha t_r)$ differ very little from each other at the border of resonance (3%) whereas for $\alpha/\omega = 10^{-1}$ the

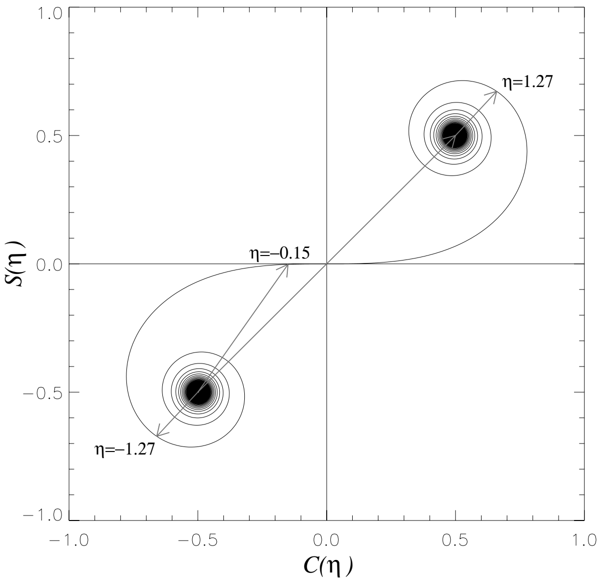

Figure 2. The Cornu spiral (plot of the Fresnel integrals $C(\eta)$ and $S(\eta)$, $\eta = (\alpha\omega/\pi)^{1/2}t$) visualizes the growth of amplitude (length of the arrows) of a harmonically driven linear oscillator undergoing resonance at $t = \eta = 0$. Resonant excitation happens in the interval $|\eta| \leq 1.27$.

difference is 33%. Nevertheless the Fresnel integrals yield very satisfactory results also in this case as shown in Fig. 3 for $x(t)$.

For determining the factor of resonant growth of $x(t)$ and the amount of energy absorbed by the oscillator we observe that outside the resonance width any adiabatic variation of $\omega_0(t) \neq \omega$ under an adiabatically varying driver $\hat{a}(t)$ may influence the shape of the two spirals of Fig. 2 but has no effect on the resonance segment in between ($|\eta| < \eta_r$). Hence, the growth of $x(t)$ for $\omega_0(t) = \omega \exp(-\alpha t_r)$ is (nearly) the same as for $\omega_0(t)$ from (12), provided $\alpha/\omega \leq 0.3$ as deduced from Fig 3. After the driver is switched off adiabatically $x(t \to \infty)$ points to the center of the upper spiral at $C(\infty) = S(\infty) = 1/2$. This position also indicates the final energy $e_a(\infty)$ irreversibly gained by the oscillator after crossing the resonance point if its frequency is kept at $\omega_0(t_r) = \omega_f =$ const. Equation (16) yields the following quantities for resonant and asymptotic amplitude increase κ_r, κ_∞, and stored energy $e_a(\infty)$,

$$\kappa_r = \frac{\hat{x}(\eta_r)}{\hat{x}(-\eta_r)} = 7.0, \qquad \kappa_\infty = \frac{\hat{x}(\infty)}{\hat{x}(-\eta_r)} = 6.0, \tag{19}$$

$$e_a(\infty) = \frac{1}{2}\omega^2\hat{x}^2(\infty) = \frac{\pi\hat{a}^2(\eta = 0)}{4\alpha\omega}.$$

For $\omega_0(t > t_r) \to 0$ the final energy depends on how rapidly the parabolic potential flattens: if the number of turning points is infinite $e_a(\infty)$ is zero, if it is finite the particle escapes with finite kinetic energy. We conclude by observing that if the oscillator is switched off adiabatically before $-t_r$ it returns to its starting position $C = S = -1/2$; if it is adiabatically switched off after $+t_r$ and $\omega_0(t_r) = \omega_f$ is kept constant it has made the irreversible transition from the center of the lower spiral to the center of the upper spiral in Fig. 2. A linear oscillator can gain irreversible energy (absorption) under ballistic (collisional) excitation or, adiabatically, by crossing a resonance.

3. Adiabatic excitation of a nonlinear oscillator

The main difficulty in understanding frictionless interaction of intense laser beams with dense matter (solids, clusters, aerosols, dust) has its origin in the fact that the eigenfrequency of ionized matter ω_p is typically ten times higher than the driving laser frequency. It is evident that for this reason a linear oscillator fails to explain the phenomenon of collisionless heating.

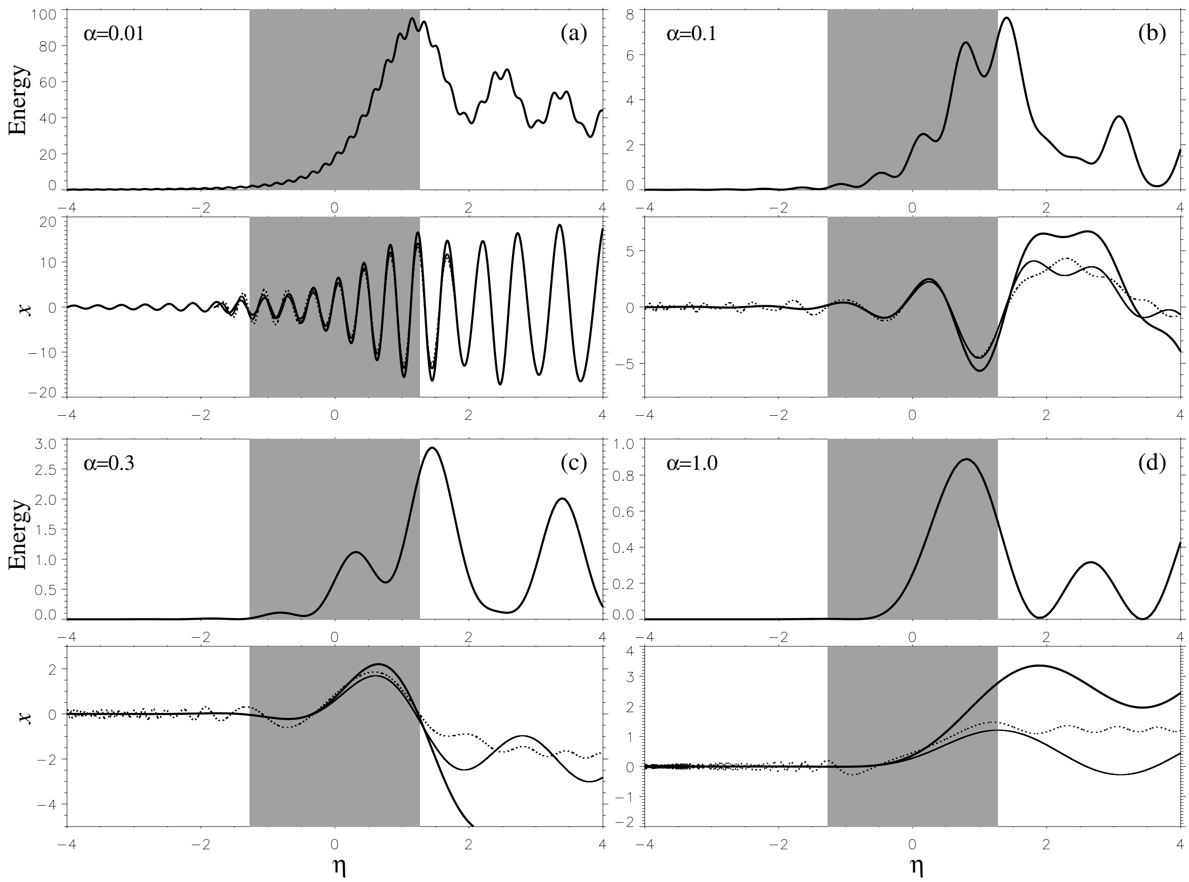

Figure 3. Total energy $\omega_0^2(t)x^2(t)/2 + \dot{x}^2(t)/2$ and trajectory $x(t)$ from the numerical solution of (8) vs η for $\hat{a} = \omega = 1$ and $\alpha = 0.01$ (a), 0.1 (b), 0.3 (c), and 1.0 (d), all drawn solid and bold. For comparison $x(t)$ according (10) (thin solid curves) and (13) (dotted) are included. The resonance region $|\eta| < \eta_r = 1.27$ is shaded gray. Dotted graph is relevant only in the resonance region. Equation (10) is a valid approximation in the shaded region for $\alpha\omega \leq 0.3$. The discrepancy in $x(t)$ at $\eta > \eta_r$ is partly due to a constant drift of the particle, not included in (10). The modulations in energy can be qualitatively understood with the help of the Cornu spiral.

An undamped nonlinear oscillator may exhibit properties differing in many respects from its linear counterpart. For our purpose here its most important difference is the dependence of the eigenperiod T_0 on the excitation level, i.e., on the amplitude. In the case of the very general nonlinear oscillator (3) T_0 is given by $\int \mathrm{d}t = \int \mathrm{d}s/v$, v particle velocity, or

$$T_0 = \oint \frac{\mathrm{d}s}{\left\{\left(\frac{2}{m}\right)[V_0 - V(\boldsymbol{x})]\right\}^{1/2}}, \qquad V_0 = \max V(\boldsymbol{x}). \tag{20}$$

The integration is taken along the orbit $\boldsymbol{x}(t)$, with the line element ds. In the following we limit ourselves to oscillations in one dimension. Let $V(x)$ be the potential associated with the restoring force $f(x)$ so that $f(x) = -\partial_x V(x)$. If the graph of $V(x)$ stays inside the parabola $\omega_0^2 x^2/2$ the eigenperiod decreases with the amplitude; if however it widens compared to the parabola its eigenperiod increases with increasing level of excitation. This latter case is of particular interest because Coulomb systems exhibit such a characteristics owing to the $1/r$-dependence of the Coulomb potential at large charge separation and, in concomitance, at a fixed driver period the nonlinear system may enter into resonance when excited to high amplitude. This property opens the new possibility to couple appreciable amounts of energy by adiabatic excitation into such systems originally out of resonance. Since even the shortest laser pulse contains several oscillations ballistic excitation is not possible, in a locally plane wave not even in principle, regardless of how short the electromagnetic pulse is (see next Section).

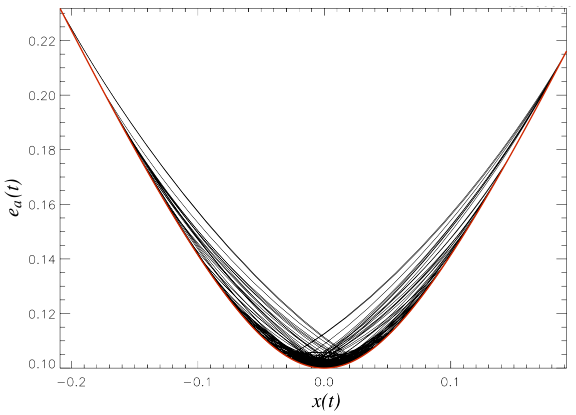

Figure 4. Electron trajectory in the xe_a-plane, $e_a(t) = V(x(t)) + \dot{x}^2(t)/2$, for the case where the particle does not cross the nonlinear resonance $T = T_0$ with T_0 according (23), i.e., at $x_0 \approx V(x_0) = 4$. Equation (22) was solved numerically for $\epsilon = 0.1$, $\hat{a}(t) = a_0 \sin^2[\omega t/(2n)]$, $a_0 = -0.84$, $n = 40$ cycles, $\omega = 0.555$, and $x(0) = \dot{x}(0) = 0$. Almost no energy remains in the system after the end of the pulse, $e_a(\infty) \approx 0$.

Owing to its relevance to collisionless heating large amplitude oscillations of a neutral plasma layer are studied. The ions are supposed to be fixed and to occupy uniformly a plane layer of thickness d. The electrons are uniformly distributed over a distance $a \geq d$ in order to allow for thermal expansion due to finite electron pressure. The electrons oscillate according to the following equations of motion,

$$\begin{aligned} \ddot{x} + \omega_p^2 x &= -eE_d(t)/m_e \quad \text{for} \quad |x| \leq (a+d)/2, \\ \ddot{x} + \frac{a+d}{2}\omega_p^2 \operatorname{sgn} x &= -eE_d(t)/m_e \quad \text{for} \quad |x| > (a+d)/2. \end{aligned} \tag{21}$$

Without loss of essential aspects these two equations can be approximated by one describing the motion in a potential $V(x) = (\epsilon^2 + x^2)^{1/2}$ with ϵ a parameter,

$$\ddot{x} + \frac{x}{(\epsilon^2 + x^2)^{1/2}} = \hat{a}(t) \cos \omega t. \tag{22}$$

Once the particle gained an energy $e_a \gg \epsilon$, $V(x) \approx |x|$ holds, and the eigenperiod results from (20) as

$$T_0 = 4(2x_0)^{1/2} \tag{23}$$

where $\pm x_0$ are the two turning points for a given total energy $V(x_0)$. For excursions $x \ll \epsilon$, on the other hand, the potential reads $V(x) \approx \epsilon + x^2/(2\epsilon)$ with the constant eigenfrequency $\omega_0 = \epsilon^{-1/2}$.

In all following calculations the driver amplitude $\hat{a}(t)$ is a $\sin^2$-pulse covering 40 harmonic oscillations of frequency ω. For convenience the scale of the excursion $x(t)$ is fixed such that resonance occurs at $x_0 = 4$ which implies $\omega = \sqrt{2}\pi/8 = 0.555$. Excitation much below resonance is shown in Fig. 4 for the evolution of e_a vs $x(t)$. After the pulse is over $e_a(t \to \infty) = 1.6\%$ of its maximum value during the pulse. When the oscillator undergoes a resonance the situation changes drastically, as illustrated by Fig. 5. In (a) the driver $-a(t)$, the excursion $x(t)$, and the energy $e_a(t) = V(x(t)) + \dot{x}^2(t)/2$ are plotted. The resonance zone is crossed approximately during one cycle, and the change of phase between driver and position $x(t)$ by π is clearly seen. The stored energy fraction amounts to $e_a(\infty)/\max e_a(t) = 52\%$. As expected from an adiabatic pulse and the structure of the Cornu spiral, after resonance the energy $e_a(t)$ is modulated with an asymptotic value $e_a(\infty) \approx (\max e_a + \min e_a)/2$. In (b) the dynamics $e_a(x(t))$ is shown. The asymptotic state $e_a(\infty)$ at $e_a = 9.4$ is easily recognized from the horizontal trajectory after the pulse is over (free oscillations in the potential $V(x)$).

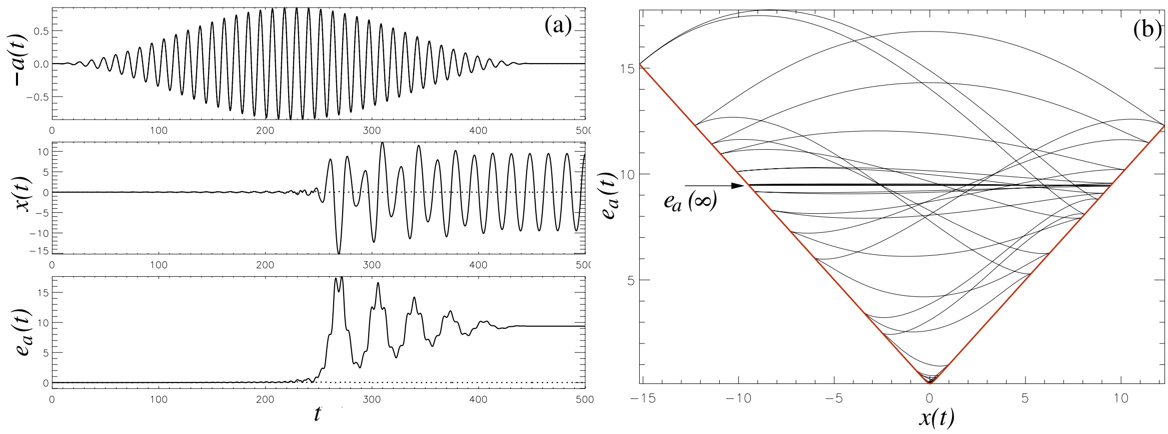

Figure 5. Numerical solution of (22) for $a(t) = a_0 \sin^2[\omega t/(2n)] \cos \omega t$, $n = 40$, $\omega = 0.555$, $a_0 = -0.85$, and $\epsilon = 0.1$. Panel (a) displays (from top to bottom) driver $-a(t)$, position $x(t)$, and energy $e_a(t)$. Although the driver amplitude is only 0.01 above the value of Fig. 4 the particle now crosses the resonance at $x_0 \approx V(x_0) = 4$, leading to an irreversible energy gain. Panel (b) shows the electron trajectory in the xe_a-plane. The final energy $e_a(\infty)$ lies well above $V(x_0) = 4$.

When $e_a(\infty)$ is plotted as a function of the driver amplitude $-a_0$ a very significant picture appears (Fig. 6): at resonance (corresponding to $x_0 = 4$) $e_a(\infty)$ undergoes a sudden jump by 3 orders of magnitude, except some rare "pathological" cases. One of them is shown in Fig. 7a.

Another type of rare cases is presented in Fig. 7b,c, this time obtained in an asymmetric potential. The particle continues to absorb a significant amount of energy after passing the resonance. This is due to the fortunate coincidence that the increasing particle bounce velocity keeps the particle in resonance during the passage from one turning point to the subsequent one. The final horizontal trajectory in Fig. 7c is now located close to $\max e_a(t)$.

The "phase transition" from below resonance to above resonance is independent of the particular shape of the potential. In fact, with the asymmetric potential of Fig. 7c, Fig. 8 is obtained which reproduces all essential aspects of Fig. 6 for the symmetric potential (note the different scaling), in particular the jump by more than three orders of magnitude between $-a_0 \approx 0.5$ and 1.0.

Owing to its relevance for collisionless heating of clusters and sprays the resonance behavior of two oscillating spheres of electrons and ions has also been investigated. In this case the potential is a polynomial in the separation coordinate r of powers -1, 2, 3, and 5. Again, the picture analogous to Figs. 6 and 8 is qualitatively the same. As a consequence of higher nonlinearity and higher dimensionality (motion in two directions) the discontinuity at resonance is one order of magnitude less but still high (an abundant factor of 10^2) and local structures are less pronounced (less "pathology"), however, still present. This proves our assertion that significant energy gain from an adiabatic driver requires the existence of resonances.

For its relevance to numerous applications (e.g., field ionization by intense laser beams [6], generation of fast electron and ion jets from gases and solid targets [7]) open or half open potentials are of interest.

If the barrier $V(\pm\infty)$ is well above the threshold for resonance $V_{\rm res}$ only very few particles are expected to escape (e.g., such of type Fig. 7b). If however $V(\pm\infty) \lesssim V_{\rm res}$ all particles which are resonant in the associated closed potential do escape (an example is given in Fig. 9), except very few which may recombine.

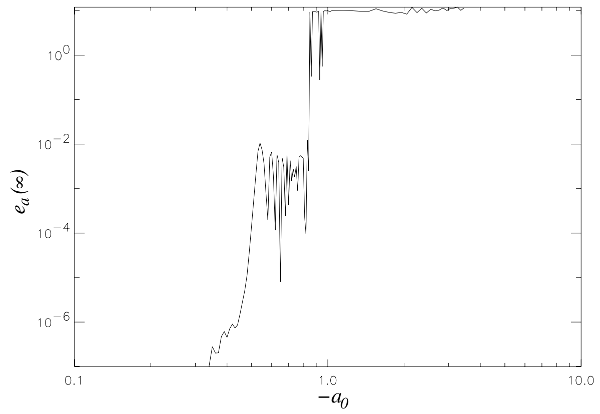

Figure 6. Final energy $e_a(\infty)$ as a function of the driver amplitude $-a_0$ for the system (22) with $\omega = 0.555$, $n = 40$, and $\epsilon = 0.1$. For driver amplitudes $-a_0 < 0.84$ the particle remains in the regime where $T_0 < T$. For $-a_0 \geq 0.85$ the particle crosses the resonance $T_0 = T$ in most cases, and $e_a(\infty)$ is about three orders of magnitude larger. However, the absorbed energy does not increase further with the driver amplitude. In a few isolated, pathological cases, a significant amount of the absorbed energy may be given back to the field also for $-a_0 > 0.85$. An example is given in Fig. 7.

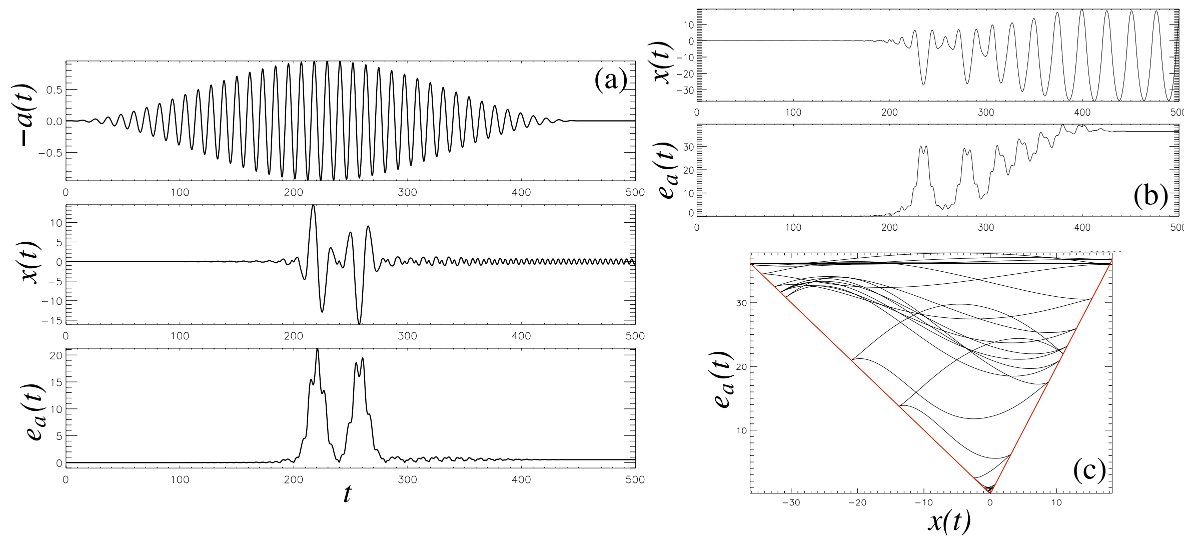

Figure 7. Two examples for isolated, "pathological" cases. Plot (a) refers to the symmetric case (22) for $-a_0 = 0.95$, all other parameters as described in the caption of Fig. 6. From the e_a-plot one infers that the resonance at $e_a = 4$ is crossed four times so that the particle finally ends up below resonance, giving almost all its energy adiabatically back to the field ("2π pulse"). Plots (b) and (c) refer to the same calculation for an asymmetric potential whose RHS part is twice as steep as the LHS part. The driver amplitude was $-a_0 = 0.97$. Under these particular conditions the particle continues to absorb energy after passing the resonance around $t = 210$. This is due to the fortunate coincidence that the increasing particle bounce velocity keeps the particle in resonance during the passage from one turning point to the subsequent one (multiple "echoes").

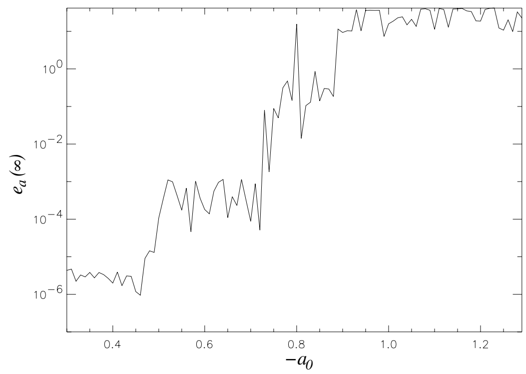

Figure 8. Final energy $e_a(\infty)$ as a function of the driver amplitude $-a_0$ for the asymmetric potential of Fig. 7c. Only the transition regime from underresonant ($T_0 < T$) to overresonant ($T_0 > T$) behavior is shown. The basic features are very similar to the result for the symmetric potential in (6).

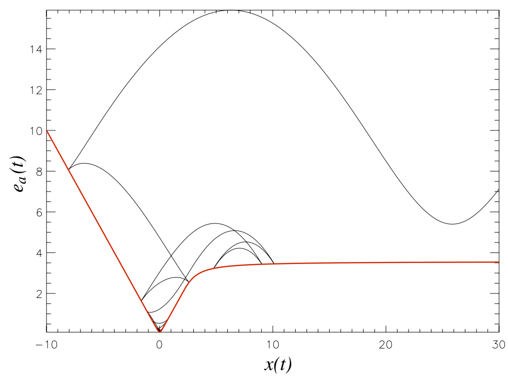

Figure 9. Particle trajectory in the xe_a-plane for an open potential and driver amplitude $-a_0 = 0.9$ (other laser parameters as in the previous figures). The particle escapes not before passing through the resonance of the corresponding closed potential (at $e_a = 4$) although the potential is asymptotically open already for $e_a = 2 + \pi/2 < 4$. Consequently, the plot of $e_a(\infty)$ vs $-a_0$ (not shown) is very similar to Fig. 6.

4. Summary and concluding remarks

Collisionless absorption of intense laser pulses ($\lesssim 100$ fs) on the surface of plane solid targets or clusters is solved by numerical simulations but still an unsolved problem physically. $\boldsymbol{j} \times \boldsymbol{B}$-heating [8], Brunel effect (wave breaking, [9]) or laser dephasing heating [10] have been invoked. At closer inspection none of them can explain how "free" electrons can irreversibly absorb energy from a laser pulse several, typically 3–10, cycles long. As we have shown, only resonant particles can absorb energy from adiabatic drivers. Here one could make two objections: thermal electrons crossing the very thin skin layer of thickness $d \ll \lambda$, λ laser wavelength, are subject to ballistic excitation (i), or driven in a time-dependent potential $V(x,t)$ (ii). In the first case heating is possible in principle, as shown in Sec. 2, but not in the case of a locally plane electromagnetic pulse owing to the conservation of the canonical momentum in the direction of laser polarization. The second variant does not work either because the time-dependent potential has its only origin in the space charge of the electrons whose time-dependence is centered around $T = 2\pi/\omega$ with $\omega \ll \omega_p$. Of course, there is some contribution from higher harmonics present, however it is much weaker than the fundamental oscillation at the laser period.

The present investigations have shown that in the absence of dissipation (collisions) particles can absorb energy either by impact (ballistic) excitation or by being driven into resonance. The model of the linear oscillator with time-dependent eigenfrequency is a useful tool for studying special nonlinear phenomena [4] or as a guide to understand qualitatively the resonance behavior of nonlinear oscillators.

Acknowledgments

D.B. acknowledges support by the Deutsche Forschungsgemeinschaft within the Heisenberg program.

References

[1] Mulser P and Saemann A (1997) *Contrib. Plasma Phys.* **37** 217

[2] Posthumus J (ed) 2001 *Molecules and Clusters in Intense Laser Fields* (Cambridge: Cambridge University Press) ch 5–7

[3] Ruhl H and Mulser P 1995 *Phys. Lett.* A **205** 388

[4] P. Mulser 1991 *Handbook of Plasma Physics*, ed Rosenbluth M N and Sagdeev R Z (Amsterdam: North-Holland) p 448

[5] Born M and Wolf E 1988 *Principles of Optics* (Cambridge: Cambridge University Press) p 480

[6] Bauer D 1997 *Phys. Rev.* A **55** 2180; Bauer D and Mulser P 1999 *Phys. Rev.* A **59** 569

[7] Mangles S et al 2004 *Nature* **43** 535; Hegelich M et al 2003 *Phys. Rev. Lett.* **89** 085002; Kaluza M et al 2004 *Phys. Rev. Lett.* **93** 045003

[8] Kruer W L and Estabrook K 1985 *Phys. Fluids* **28** 430

[9] Brunel F 1987 *Phys. Rev. Lett.* **59** 52; Brunel F 1988 *Phys. Fluids* **31** 2714

[10] Jungreuthmayer C H et al 2004 *Phys. Rev. Lett.* **92** 133401